

# Design of a Dual-Frequency Patch Antenna for Small Satellites

*A. Lovascio\*, M. Grande\*, A. D'Orazio\* and V. Centonze\*\**

*\*DEI, Dipartimento di Ingegneria Elettrica e dell'Informazione, Politecnico di Bari*

*Via G. Amendola 126/B, 70126, Bari, Italy*

*\*\*Space Instrument & Avionic Division, Sital S.p.A.*

*Via San Sabino 21, 70042, Mola di Bari, Italy*

## Abstract

In recent years, we are witnessing an exponential growth in the use of small satellites that are extremely attractive from cost reduction point of view because of their small size. However, small size makes complicated installing two antennas at different operating frequencies, especially if the frequencies have high frequency ratios (S- and X- band). In this paper, we report the design of a dual-frequency patch antenna that exploits shorting pins to optimize the frequency ratio. The effect of presence of the metal pins on antenna performance has been analyzed showing the correlation between their geometry placement and impedance matching.

## 1. Introduction

In recent years, researchers from all over the world are carrying on studies regarding 5G technologies, especially in antenna design field. The patch antennas are devices particularly suitable for this new emergent technology because, thanks to the ease of manufacturing, they provide interesting perspective in terms of alternative geometries that are able to operate at two or more frequencies.

The dual-frequency capability can find a relevant position also in the market of the small satellites. The small satellites are becoming more and more widespread in the aerospace industry because, thanks to their small size and weight, they allow to reduce the launch costs by encouraging the implementation of a wide set of space applications. Several studies have been carried out on new technologies for the size reduction of microwave devices, such as radio-frequency filters based on fractals [1], and systems such as the Telemetry Tracking and Command (TT&C) based on commercial off-the-shelf components [2], [3].

The small size of these satellites can, of course, affect even the antenna design. According to the final application, the satellite may need to transmit and/or receive signals at two different frequency bands, even much spaced to each other. A typical scenario could be a satellite designed for the earth observation that has on board a TT&C for the service communications. For example, the European Cooperation for Space Standardization (ECSS) allows to allocate the S-band for the telemetry and telecommand operations and the X-band for the earth observation [4]. In order to exploit both bands at the same time, two different antennas could be necessary. Of course, installing two antennas instead of one that has a dual-frequency capability requires more effort in solving encumbrance and size issues, as well as higher costs. For this reason, many studies of patch antennas able to transmit two or more frequencies are available in literature [5-8].

Although the literature on dual band antennas is wide and extremely current, few studies are present on antennas with a high ratio between the two resonance frequencies. The frequency ratio is related to the approach used to create the dual-frequency capability. For example, in [9] the slots are used to realize the dual-frequency capability. However, the slots have geometric limitations related to the presence of unwanted spurs on the reflection coefficient. The spurs appear if the antenna is designed in order to meet a high frequency ratio using the slot-based approach. This approach works only if certain constraints are satisfied, such as a low frequency ratio [10].

An interesting configuration of high frequency ratio antenna is described in [11]. The antenna exploits a reactive loading realized by means of a metal pin that behaves as short-circuit between the top metal patch and the underlying ground plane. The solution proposed by the authors in [11] allows to reject all spurs and realize a double frequency resonant antenna operating at L- and X- band for remote sensing application.

In this paper, a dual-frequency patch antenna, exploiting shorting pins and operating at S- and X-band, has been designed. Using the finite element method (FEM), the antenna size has been optimized in order to irradiate at 2.2-

2.29 GHz and 8.03-8.4 GHz to be compliant to the frequency allocation foreseen by ECSS for service communications and earth observation applications. Initially, the frequency requirements have been obtained by changing the geometric size of the antenna. We have observed that the shorting pin has a great impact on the antenna performance, especially from the point of view of impedance matching. Extending the results discussed in [11], we have performed a parametric analysis investigating the correlation between the shorting pin and the antenna performance. We have verified that the shorting pin not only affects the impedance matching and the value of the resonance frequencies, but it allows also to tune the resonance frequencies without changing the effective size of the antenna.

The role of the shorting pin was further deepened by designing a second patch antenna based on two metal pins. The presence of the second pin, respecting appropriate geometric conditions, makes the antenna resonant at single frequency. The novel antenna behaves as a single radiator at higher frequency. The lower resonance frequency is no longer present in the reflection coefficient spectrum. The second pin could be electronically realized, paving the way to possible applications in 5G communications.

## 2. Antenna Description

### 2.1 One-pin Antenna

Fig. 1 shows the sketch of the one-pin antenna with the top metal patch (blue) and the underlying ground plane (white). The antenna has been designed using a Rogers RT/duroid 5880 substrate (1.58 mm thick). The antenna has a footprint  $L \times W$  equal to 40.75x33.25 mm. The metal patch is constituted of two different forms: an external rectangular shape that contains an inner circular shape. The internal shape is separated from the external one by a circular slot. The two parts are connected along the x-axis direction by a copper bridge, having  $D$  width, short-circuited to ground plane through a thin metal pin. The values of the geometrical parameters of the antennas are reported in Tab.1.

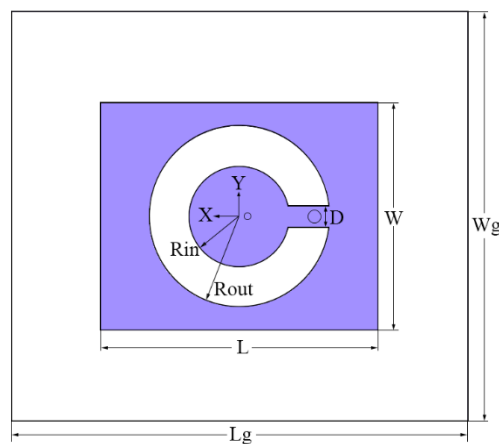


Figure 1: Geometry of the patch antenna based on one metal pin inside a copper bridge.

The two metallic parts can be seen as independent radiators that operate at their resonance frequency since the metal pin acts as a “metal boundary” between two forms. The rectangular patch due to its larger size resonates at a lower frequency, which has been tuned to fall within 2.2-2.29 GHz. Conversely, the circular patch, being smaller, resonates at a higher frequency, which has been designed to fall within the 8.03-8.4 GHz range. Since the copper bridge realizes a connection from the internal and external shape, the entire structure can be powered by a single coaxial probe that makes resonant the two frequencies at the same time. Unlike the conventional patch antenna, regardless of the shape, the position of the probe feed does not appreciably affect the impedance matching of the structure because of the presence of the metal pin inside the copper bridge. Therefore the metal pin not only avoids that two resonators influence each other bringing to the generation of unwanted spurious resonance frequencies but also is the only responsible for the impedance matching. The parametric analysis described in Section 3 reports in detail the correlation between the geometric properties of the pin and the antenna performance.

Table 1: Geometric parameter of the patch antenna

	Symbol	Value	Unit
Ground plane length	$L_g$	67	mm
Ground plane width	$W_g$	60	mm
Antenna length	$L$	40.75	mm
Antenna width	$W$	33.25	mm
Inner circular shape radius	$R_{in}$	7.4	mm
Circular slot radius	$R_{out}$	13.3	mm
Copper bridge width	$D$	2.75	mm
Metal first pin position <sup>a</sup>	$X_{pin1}$	-11	mm
Metal second pin position <sup>b</sup>	$X_{pin2}$	12	mm
Metal pin radius	$R_{pin}$	0.9	mm
Probe feed position	$X_{feed}$	-1.5	mm

<sup>a</sup>Referred to one-pin geometry

<sup>b</sup>Referred to two-pin geometry

## 2.2 Two-pin Antenna

Since the metal pin has a relevant function in antenna performance, a new configuration of the patch antenna assisted by two pins has been designed. The geometry is depicted in Fig. 2. The antenna is composed of two copper bridges that link the internal shape with the external one, making the structure symmetrical respect to the y-axis. The new second bridge has a second metal pin that realizes a metal link with the ground plane. From the electrical point of view, even the second pin acts as a metal boundary and its presence totally isolates the external rectangular patch from the internal one. The external shape does no longer irradiate at its resonance frequency and entire antenna behaves as it was a single-frequency antenna.

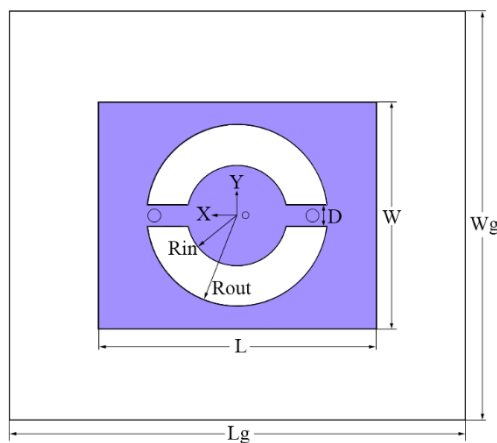


Figure 2: Sketch of the patch antenna based on two metal pins inside the copper bridges.

### 2.3 Antenna Design

The parametric analysis has been performed starting from the geometry whose parameters are reported in Tab. 1. Such parameters have been derived by full-wave simulations using COMSOL Multiphysics finite element method.). Fig. 3 shows the wideband reflection coefficient ( $S_{11}$ ) of the patch antenna assisted by one metal pin. The dual-frequency resonant operation has been obtained.

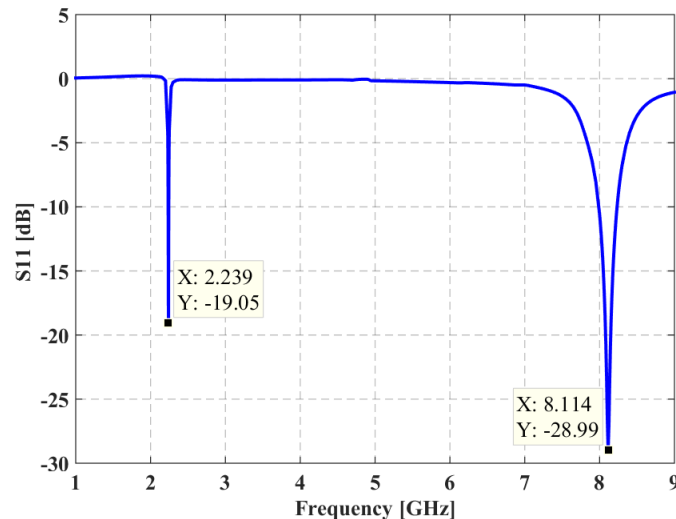


Figure 3: Reflection coefficient for the one-pin patch antenna.

The low resonance frequency at 2.24 GHz is within 2.2-2.29 GHz operating frequency range; the high resonance one is at 8.114 GHz within 8.03-8.4 MHz operating frequency range. Moreover, the spectrum does not show any spurs caused by the contemporary presence of two different shapes thanks to the metal pin that acts as a reactive loading for the spurs. The radiation pattern of the antenna at two resonance frequencies is plotted in Fig. 4 which shows that maximum antenna gain is about 6 dBi for low resonance frequency and 8 dBi for high resonance frequency both in the H-plane and E-plane.

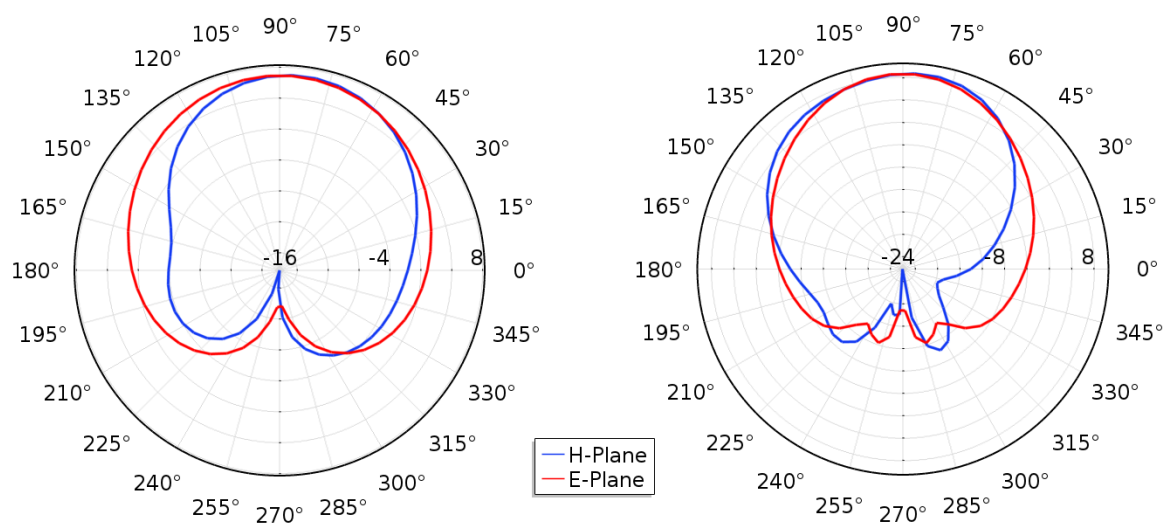


Figure 4: Radiation pattern of the one-pin patch antenna at 2.24 GHz (left) and 8.114 GHz (right) frequency.

The behavior of the metal pin as metal boundary is shown in Fig. 5 that compares the reflection coefficient of the two-pin antenna with that calculated for the one-pin antenna.

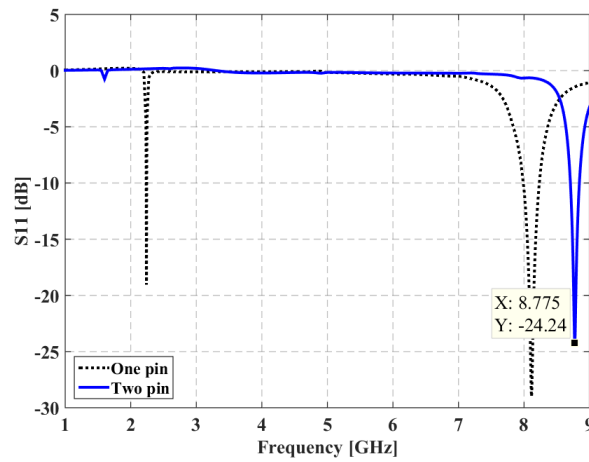


Figure 5: Reflection coefficient  $S_{11}$  for the one-pin antenna (dashed line) and the two-pin patch antenna (solid line).

The antenna assisted by two pins has only a resonance frequency located at 8.775 GHz. The low resonance frequency is no longer present, suggesting us that only the inner circular shape has irradiated an electromagnetic field, as shown in Fig. 6.

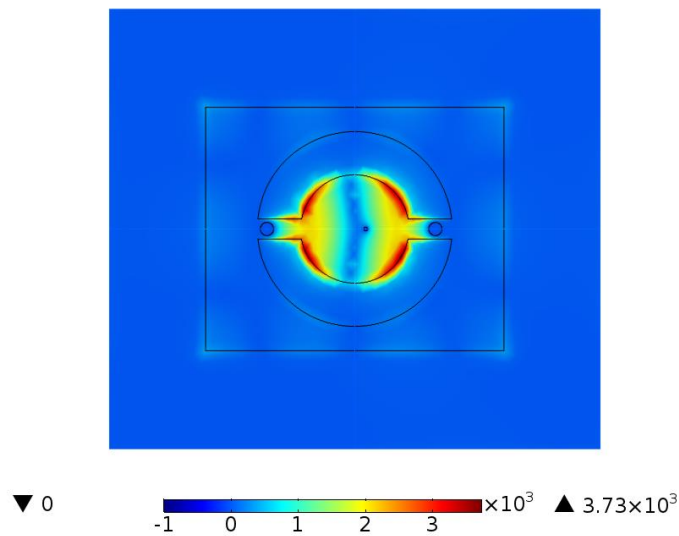


Figure 6: Absolute magnitude of the current density ( $A/m^2$ ) at 8.775 GHz of the two-pin patch antenna.

The radiation pattern at high resonance frequency for the two-pin geometry has been also analyzed in Fig. 7 showing a maximum antenna gain of about 6 dBi.

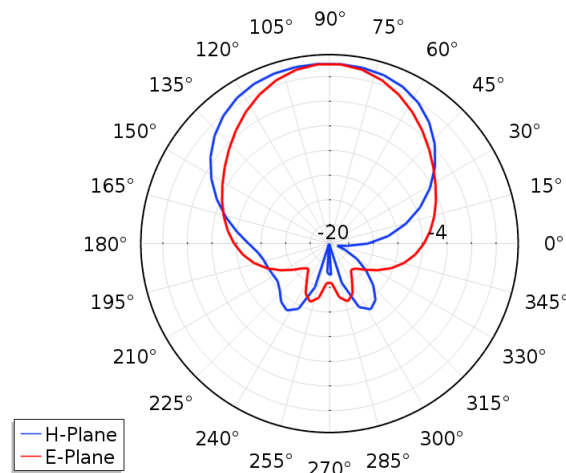


Figure 7: Radiation pattern of the two-pin patch antenna at the resonance frequency equal to 8.775 GHz.

### 3. Parametric Study

#### 3.1 One-Pin Antenna Results

A parametric analysis has been performed on both the configurations in order to better understand how resonance frequencies and impedance matching are related to the presence of the pins. As discussed in Section 2 since the pins behave as metal boundaries, they affect the impedance matching of the antenna more than the feed position. The impedance matching has been analyzed for both the resonance frequencies, starting from the one-pin geometry and changing all the parameters related to the pin, such as the copper bridge width, the pin position and its radius. Fig. 8 shows the  $S_{11}$  parameter for different values of the copper bridge width  $D$ .

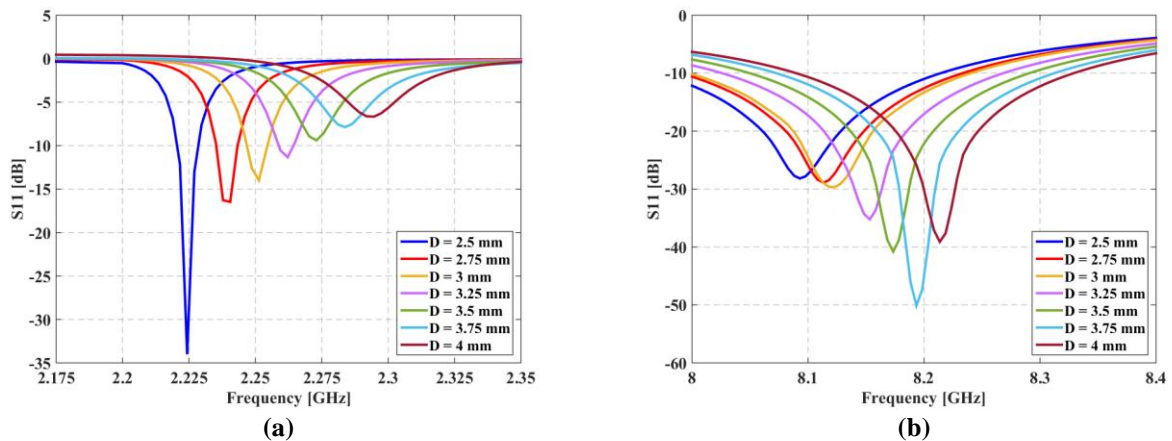


Figure 8: Reflection coefficient of the one-pin antenna for different value of  $D$  parameter at low (a) and high (b) resonance frequency.

Fig. 8 shows that low resonance frequency strongly depends on  $D$  parameter while the impedance matching is always good for all values of  $D$  for the high resonance frequency. By increasing the  $D$  value, the absolute value of  $S_{11}$  decreases causing a worse antenna matching. In addition, a frequency shift on the resonance frequency has been observed of about 70 MHz and 120 MHz at low and high resonance frequencies, respectively.

Fig. 9 depicts the  $S_{11}$  parameter for different values of the pin radius  $R_{pin}$ .

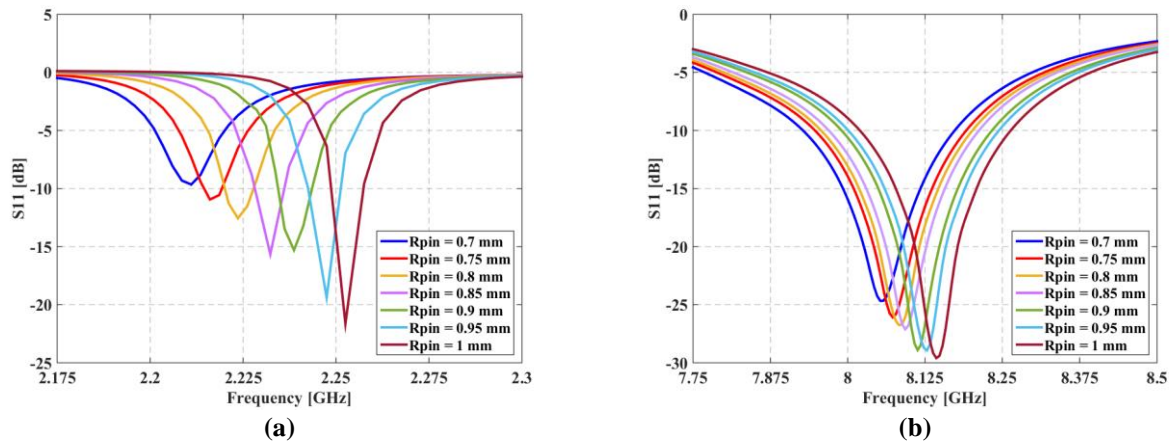


Figure 9: Reflection coefficient of the one-pin antenna for different value of Rpin parameter at low (a) and high (b) resonance frequencies.

The figure shows once again that the low frequency impedance matching strongly depends on the pin while its presence is not significant for the high frequency where the impedance matching is always good for all considered value of the Rpin parameter. However, by increasing the pin radius, the absolute value of  $S_{11}$  parameter increases improving the impedance matching at low frequency. In other words, the graphs in Fig. 8(a) and Fig. 9(a) suggest us that the impedance matching is related to the gap between the pin and the bridge external edge. If this gap decreases, the antenna matching at low frequency improves.

By changing the Rpin parameter, a frequency shift is also observed. The shift is about 42 MHz for the low and 90 MHz for the high resonance frequencies.

Finally, Fig. 10 plots the  $S_{11}$  parameter of the antenna for different values of the pin position Xpin1, the distance from the antenna center along the x-axis according to reference system depicts in Fig. 1.

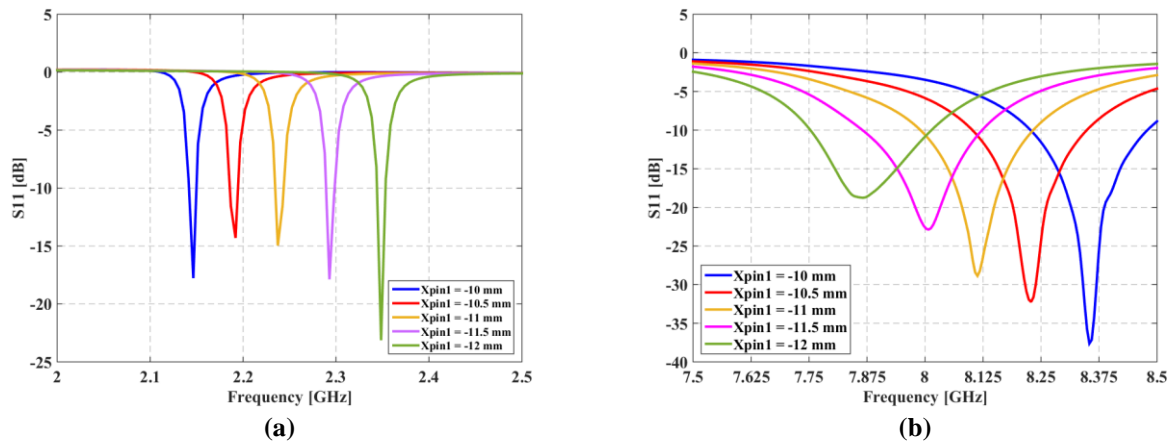


Figure 10: Reflection coefficient of the one-pin antenna for different value of Xpin1 parameter at low (a) and high (b) resonance frequencies.

Fig. 10 shows that the pin position has a great impact on the resonance frequency both for the low and the high one. The lower resonance frequency is shifted of about 200 MHz and the higher one of about 490 MHz. Instead, the impedance matching is not affected by the Xpin1 parameter.

An interesting result reported in Fig. 10a is that the amount of frequency shift for 1 mm in the variation of the pin position is as wide as the entire operating interval. This observation is better highlighted in Fig. 11 that depicts the  $S_{11}$  parameter for Xpin1 = -11 mm and Xpin1 = -12 mm using the same Rpin range considered in Fig. 9.

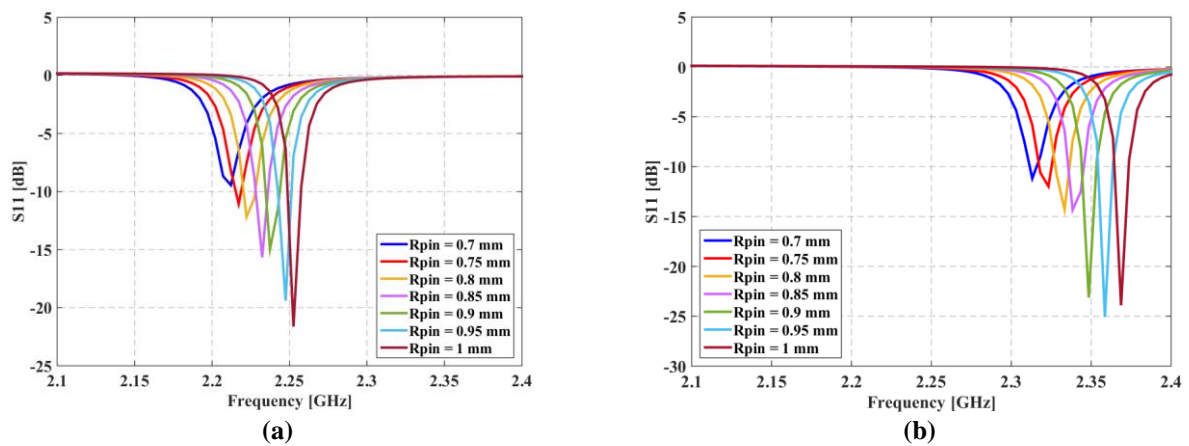


Figure 11 : Reflection coefficient of the one-pin antenna for different value of  $R_{pin}$  parameter at  $X_{pin1}=-11$  mm (a) and  $X_{pin2}=-12$  mm (b).

Fig. 11 shows that, moving from  $X_{pin1}=-11$  mm to  $X_{pin1}=-12$  mm, the interval of resonance frequency variation caused by  $R_{pin}$  changes from 2.2-2.29 GHz (the original operating frequency range) to 2.3-2.39 GHz. The intervals of resonance frequency variation are totally disjointed. This observation can be exploited to make the antenna adjustable at more levels and to prevent the uncertainty due to fabrication tolerance. For example, the two 2.2-2.29 GHz and 2.3-2.39 GHz ranges could be exploited for two antennas, one used to transmit and the other one used to receive. The two antennas would be exactly the same, they would have the same size and shape. From the industrial manufacturing point of view, it would be enough drilling and plating a via hole with a 1 mm gap, technologically possible. Any manufacturing tolerance in the hole radius would guarantee anyhow the compliance to the operating frequency range since the resonance frequency would shift within the same interval without making issues regarding the impedance matching. In addition, the exact resonance frequency control can be technologically feasible by properly adjusting the hole radius.

### 3.2 Two-Pin Antenna Results

The parametric analysis for the two-pin patch antenna has been performed by changing the position of the second metal pin, i.e.  $X_{pin2}$ , along the x-axis keeping fixed the position of the first pin at  $X_{pin1} = -11$  mm. Both radius and the copper bridge width are exactly the same as the one-pin antenna. Fig. 12 depicts the  $S_{11}$  parameter for various values of the  $X_{pin2}$  parameter.

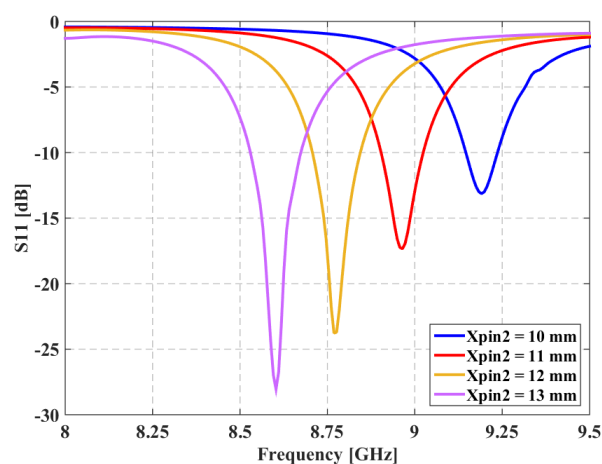


Figure 12: Reflection coefficient of the two-pin patch antenna for different position of the second metal pin.

The figure shows that the second pin affects the resonance frequency of the antenna while no relevant change on the impedance matching has been observed. For a shift of 1 mm in the pin position, there is a resonance frequency shift of about 200 MHz. The amount of this shift increases as the distance of the pin from the antenna center decreases.

For the entire interval considered for the  $X_{pin2}$  parameter, a resonance frequency shift of about 590 MHz has been obtained.

The previously observation has been done by assuming that the second pin is maintained within the bridge length, which is equivalent to satisfy the condition (1).

$$R_{in} < X_{pin2} < R_{out} \quad (1)$$

Only when the pin is within the bridge length, a gap between pin and bridge edges is formed, allowing the pin to act as a metallic barrier. For  $X_{pin2} > R_{out}$ , i.e. when the pin is outside the bridge, the pin stops behaving like a metallic boundary with an impact on the antenna performance. In order to investigate the antenna performance in this situation, wideband numerical simulations have been performed for  $X_{pin2}$  values for which the pin goes from inside to outside the bridge.

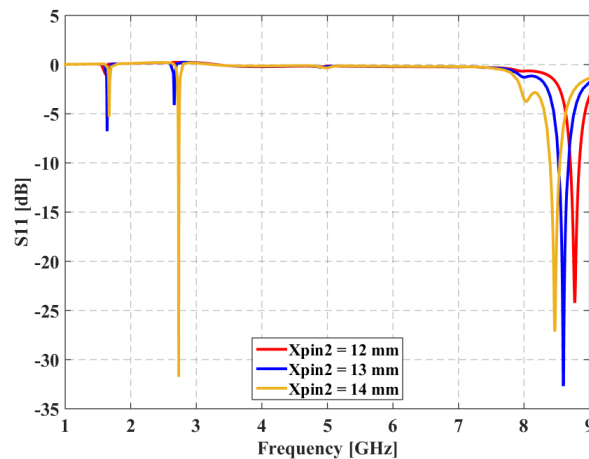


Figure 13: Reflection coefficient of the two-pin patch antenna for  $X_{pin2}$  values outside the copper bridge.

Fig.13 shows again the low resonance frequency, although the absolute value of the frequency is different respect to the one-pin antenna case. In addition, the most relevant aspect of the obtained result is the presence of a third resonance frequency located at a frequency smaller than 2 GHz. Low frequency region has been better analyzed in Fig. 14.

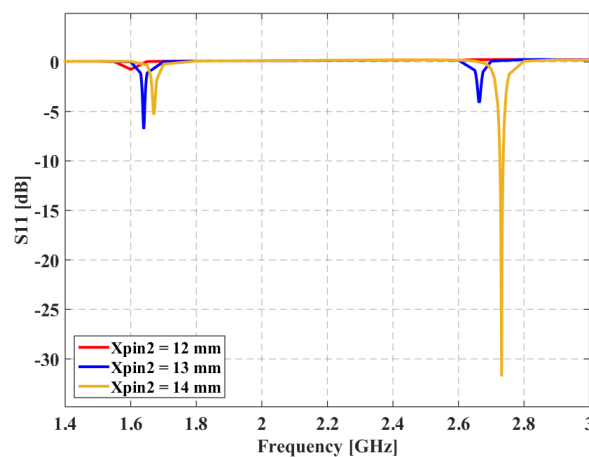


Figure 14: Reflection coefficient of the two-pin patch antenna for  $X_{pin2}$  values outside the copper bridge in the low frequency region.

The third resonance frequency is around 1.65 GHz and has a 5-6 dB absolute value of  $S_{11}$  parameter. The impedance matching is not good enough to have a good irradiation, therefore this frequency can be considered a spur. No other spur has been observed on the entire frequency range considered in Fig. 13.

## 4. Conclusion

In this paper, we report the design of double resonant patch antennas assisted by one metallic pin and two-pins. Regarding the one-pin antenna, we have shown that there is a strong correlation between the impedance matching and the gap between the pin and bridge edge for the low resonance frequency while no relevant effects have been observed for the high resonance frequency. Instead, the position of the pin affects the value of the resonance frequency both for the low and high one. For the low frequency the amount of the observed frequency shift is even greater than the same operating frequency range for which the antenna has to be compliant (2.2-2.29 GHz). By changing of 1 mm the pin position, it is possible to design an antenna that operates on different operating frequency ranges without changing the size, that is extremely attractive.

For the two-pin antenna, we have shown that according to the second pin position the antenna behaves as a dual-frequency or single-frequency antenna. If the second pin is inside the bridge, it acts as a metallic boundary isolating totally the external rectangular shape. Therefore, the antenna irradiates with only one resonance frequency (the higher one) that is generated by the inner circular shape. If the second pin is outside the bridge, the antenna does not only exhibits the dual-frequency capability but a third resonance frequency appears at frequencies lower than 2 GHz. Anyway, the second pin position affects the value of the resonance frequency. No relevant effects have been observed on the impedance matching.

The analysis highlighted interesting properties related to the reactive loading realized through a metal pin inside the antenna geometry. The metal pin not only allows to “clean” the  $S_{11}$  parameter spectrum from the unwanted spurs giving the dual-frequency capability to the antenna but also allows to control the impedance matching and the absolute value of both resonance frequencies without changing the antenna size and the shapes of its geometry.

## Acknowledgment

The Ph.D. student A. Lovascio benefits from a PhD MIUR fellowships for the 2018/2019 academic year, course XXXII, awarded within the framework of the “Programma Operativo Nazionale Ricerca e Innovazione” (PON RI 2014/2020) Axis I “Investments in Human Capital” - Action I.1- “Innovative PhDs with industrial characterization.” Funding FSE-FESR.

## References

- [1] A. Lovascio, A. D’Orazio, V. Centonze, “Effects of the coating on S-band microstrip filter performance,” published by *The Journal of Engineering (IET)* on April 15, 2019.
- [2] A. Lovascio, A. D’Orazio, V. Centonze, “Design of a TT&C Radio-Frequency Receiver for Small Satellites Based on COTS Components,” *International Conference on Aerospace Design and Optimization Technologies (ICADOT)*, May 14-15, 2019.
- [3] A. Lovascio, V. Centonze, A. D’Orazio, “Design of COTS-Based Radio-Frequency Receiver for Cubesat Applications,” *6th International Workshop on Metrology for AeroSpace (MetroAeroSpace)*, IEEE, June 19-21, 2019.
- [4] ESA-ESTEC, “Space engineering, Radio frequency and modulation,” ECSS-E-ST-50-05c, Rev.2, Requirements & Standards Division, Noordwijk, The Netherlands, October 4, 2011.
- [5] B. Yan, L. Wang, Z. Luo, D. Deng, L. Feng, “Dual-band Microstrip Antenna Fed by Coaxial Probe,” *2016 11th International Symposium on Antennas, Propagation and EM Theory (ISAPE)*, IEEE, October 2016, pp. 228-230.
- [6] K. Yu, Y. Li, X. Luo, X. Liu, “A Modified E-Shaped Triple-band Patch Antenna for LTE Communication Applications,” *2016 IEEE International Symposium on Antennas and Propagation (APSURSI)*, IEEE, June 2016, pp. 295-296.
- [7] W. C. Mok, S. H. Wong, K. M. Luk, K. F. Lee, “Single-Layer Single-Patch Dual-Band and Triple-Band Patch Antennas,” *IEEE transactions on antennas and propagation* 61.8 (2013): 4341-4344.
- [8] X. Guo, W. Liao, Q. Zhang, Y. Chen, “A Dual-band Embedded Inverted T-slot Circular Microstrip Patch Antenna,” *2016 IEEE 5th Asia-Pacific Conference on Antennas and Propagation (APCAP)*, IEEE, July 2016, pp. 151-152.
- [9] S. Maci, G. B. Gentili, P. Piazzesi, C. Salvador, “Dual-band slot-loaded patch antenna,” *IEEE Proceedings-Microwaves, Antennas and Propagation* 142.3 (1995): 225-232.
- [10] S. Maci, G. B. Gentili, “Dual-Frequency Patch Antenna,” *IEEE Antennas and propagation Magazine*, 39.6 (1997): 13-20.
- [11] S. H. S. Esfahlani, A. Tavakoli, P. Dehkoda, “A Compact Single-Layer Dual-Band Microstrip Antenna for Satellite Applications,” *IEEE antennas and wireless propagation letters* 10 (2011): 931-934.